Effect of aerosol humidification on the column aerosol optical thickness over the Atmospheric Radiation Measurement Southern Great Plains site

Myeong-Jae Jeong,[1,3] Zhanqing Li,[1] Elisabeth Andrews,[2] and Si-Chee Tsay[3]

[1] This study investigates the aerosol humidification effect (AHE) using 70 profiles of the aerosol scattering coefficients at high ($\sim$80%) and low ($\sim$40%) relative humidity (RH) levels and absorption coefficient at a low RH level obtained by a light aircraft (Cessna C-172N) over the Southern Great Plains (SGP) site from April 2003 to June 2004. The column aerosol humidification factor, R(RH), defined as the ratio of the aerosol optical thickness (AOT) at the ambient RH to that at RH = 40% throughout the column rarely exceeded 1.3 (mean, 1.09 ± 0.12) over the SGP site. However, for an atmospheric column of a constant RH = 85%, R(RH) is greater than 1.5 for the majority of cases (mean, 1.57 ± 0.28). R(RH) was fitted to a function of column RH based on this unique aerosol data set. Several methods were proposed to estimate R(RH) for use when direct measurements of R(RH) are not available. It was found that the relationship between R(RH) and aerosol extinction coefficient weighted column-mean RH works best. Performance of other methods depends on the measurements available. Sensitivity of R(RH) to a very humid (RH = 99%) layer with varying thickness values (0.1–0.3 km) is examined. The results indicate that the AHE on the AOT over the SGP site is not likely to exceed 50% on the average. The methods and results of this study may be utilized with caution to remove the AHE from the AOT retrieved from satellite or automated Sun photometer measurements, which will be useful for studies on aerosol indirect effect or quantifying cloud contamination in aerosol retrievals.

1. Introduction

[2] Aerosol optical thickness (AOT) is a vertically integrated (column) quantity whose magnitude depends on aerosol mass loading, scattering, and absorption efficiencies that are further linked with aerosol size distribution and composition. In addition to these inherent properties, AOT also varies with the ambient humidity. There have been numerous investigations concerning the relationship between relative humidity (RH) and aerosol light scattering. These include theoretical investigations [e.g., *Kasten*, 1969; *Hänel*, 1976; *Hegg et al.*, 1993; *Tang*, 1996; *Li et al.*, 2001] and field experiments using instruments on the ground and aircrafts [e.g., *Charlson et al.*, 1984; *Rood et al.*, 1987; *Kotchenruther and Hobbs*, 1998; *Li-Jones et al.*, 1998; *Kotchenruther et al.*, 1999; *Gasso et al.*, 2000].

[3] The hygroscopic property of aerosols is represented by the aerosol humidification factor (AHF), f(RH), which is defined as the ratio of the aerosol scattering coefficient at a high humidity (RH, $\sim$85%) or an ambient RH to the aerosol scattering coefficient at a low RH ($\sim$40%) [*Covert et al.*, 1972; *Rood et al.*, 1987; *Hegg et al.*, 1996]. f(RH) is normally measured using integrating nephelometers [e.g., *Charlson et al.*, 1991; *Li-Jones et al.*, 1998; *Kotchenruther et al.*, 1999; *Gasso et al.*, 2000] and was also estimated from a lidar-derived aerosol scattering profile together with a RH profile under the special condition of a well-mixed boundary layer capped by stratiform clouds [*Feingold and Morley*, 2003; *Pahlow et al.*, 2006].

[4] To date, some studies investigated the influence of humidity on the AOT [e.g., *Hegg et al.*, 1997; *Öström and Noone*, 2000] by apportioning the observed AOT among various contributing factors. However, those studies are based on the measurements made for short time periods, reporting the range of contribution of humidity effects. It is necessary to study the behavior of AOT in response to changes in humidity variables throughout the atmospheric

[1]Department of Atmospheric and Oceanic Science and Earth System Science Interdisciplinary Center, University of Maryland, College Park, Maryland, USA.
[2]Climate Monitoring and Diagnostics Laboratory, National Oceanic and Atmospheric Administration, Boulder, Colorado, USA.
[3]Laboratory for Atmospheres, NASA Goddard Space Flight Center, Greenbelt, Maryland, USA.

Table 1. Typical Altitudes of Observations Made During the In situ Aerosol Profiling Flights

Level-Leg ID	Altitude, km	Level-leg ID	Altitude
1	3.6	6	1.2 km
2	3.1	7	0.9 km
3	2.4	8	0.6 km
4	1.8	9	0.5 km
5	1.5	10[a]	5 m

[a]The data are actually taken from the Aerosol Observation System at the surface.

column using data sets incorporating the simultaneous vertical distributions of humidity and aerosols together.

[5] Quantifying the humidification effects of aerosols has important implications. For example, the correlation between AOT and cloud fraction has been reported [*Ignatov and Nalli*, 2002; *Kaufman et al.*, 2005a; *Jeong and Li*, 2005], and there have been arguments as to whether it is cloud contamination or the aerosol humidification effect (AHE), which may be defined as the changes in AOT according to the changes in aerosol scattering coefficients throughout the atmospheric column in response to RH changes therein. It is important to know the contribution of the AHE to the AOT and to quantify and eliminate any artifact because of cloud contamination (including enhanced scattering by clouds) in order to obtain true aerosol information, given large discrepancies among satellite-based aerosol products due to cloud screening [*Myhre et al.*, 2004; *Jeong et al.*, 2005].

[6] An observational study of the aerosol indirect effect (AIE) requires information about the AHE. AOT or aerosol extinction coefficients have been used as a proxy for cloud condensation nuclei (CCN) in AIE studies [*Kaufman and Nakajima*, 1993; *Nakajima et al.*, 2001; *Bréon et al.*, 2002; *Feingold et al.*, 2003]. However, AOT might not be a good proxy for CCN [e.g., *Feingold*, 2003], since AOT is a vertically integrated quantity and depends not only on the number of particles but also on humidity, size distribution, etc. Some efforts were made [*Nakajima et al.*, 2001; *Bréon et al.*, 2002] to reduce the uncertainty of using AOT as a proxy for CCN by considering the effects of aerosol size. However, little consideration has been given to account for the AHE, which has a potential for influencing the magnitude of AOT.

[7] This study attempts to quantify the effect of aerosol humidification on the AOT derived from the in situ airborne aerosol profile measurements taken over the Central Facility (CF) site in the Southern Great Plains (SGP). In section 2, the data and the methodology used in this study are described. The column AHF for AOT, which is denoted as R(RH), is defined in section 2, and its relationship with humidity variables is presented in section 3. Several methods to estimate the R(RH) are introduced and compared in section 4. Then, the sensitivity of R(RH) to a very humid atmospheric layer is tested in section 5. Summary and concluding remarks are provided in section 6.

2. Data and Method

[8] The primary source of data came from measurements taken during in situ aerosol profiling (IAP) flights made under the aegis of the Department of Energy's Atmospheric Radiation Measurement (ARM) Program. A light aircraft (Cessna C-172N) flew at nine level legs between 0.5 and 4 km above the ground level over the SGP site, collecting aerosol data every second (Table 1). The aerosol data were then averaged over each Cessna leg. The duration of the leg varies with altitude ranging from 3 to 15 min, approximately 5 min for the lowest five levels and 10 min for the highest four levels on the average.

[9] The measurements include scattering and absorption due to aerosol particles less than 1.0 μm in diameter, Dp. The configuration of the IAP measurement system is the same as described by *Andrews et al.* [2004] except for an additional nephelometer measuring aerosol scattering at high RH. The scattering coefficients were measured at blue (450 nm), green (550 nm), and red (700 nm) channels under low-humidity (RH $\sim$40%), and at 550 nm for high-humidity (RH $\sim$80%) conditions. The absorption coefficients were obtained at the green channel with RH $\sim$40%. Aerosol scattering measurements at low and high RH were made using a three-wavelength TSI nephelometer (Model TSI 3563; TSI Inc., Minneapolis, Minnesota), and a single-wavelength Radiance Research nephelometer (Model M903, Radiance Research, Seattle, Washington), respectively. A Particle/Soot Absorption Photometer (Radiance Research, Seattle, Washington) was used to measure aerosol absorption. Also observed are ambient RH, temperature, and pressure profiles. Detailed information about the measurement uncertainty and experiment was documented by *Anderson and Ogren* [1998] and *Andrews et al.* [2004], respectively.

[10] Aerosol scattering depends on RH [e.g., *Hänel*, 1976; *Hegg et al.*, 1993; *Remer et al.*, 1997]. If measurements are available at different humidity levels, the dependence of aerosol scattering on RH can be fitted to an analytic function with two to three or more parameters determined empirically [e.g., *Hänel*, 1976; *Kotchenruther and Hobbs*, 1998; *Kotchenruther et al.*, 1999]. This study uses a two-parameter fitting since the measurements are only available at two different humidity levels (low and high). The AHF for aerosol scattering, f(RH), can be defined as follows:

$$f(\mathrm{RH}) \equiv \frac{k_{\mathrm{sca}}^{a}(\mathrm{RH})}{k_{\mathrm{sca}}^{a}(40\%)}, \qquad (1)$$

where $k_{\mathrm{sca}}^{a}(\mathrm{RH})$ and $k_{\mathrm{sca}}^{a}(40\%)$ represent the aerosol scattering coefficients at a certain RH and RH = 40%, respectively. A two-parameter function has been widely used to describe the RH dependence of aerosol scattering coefficient [e.g., *Kasten*, 1969; *Hänel*, 1976; *Kotchenruther et al.*, 1999; *Andrews et al.*, 2004]:

$$f(\mathrm{RH}) = a \cdot \left(1 - \frac{\mathrm{RH}(\%)}{100}\right)^{-b}, \qquad (2)$$

where a and b are the parameters to be determined from the scattering coefficients measured at low and high RHs. One may then estimate the scattering coefficients of aerosols at any humidity using equation (2). f(RH) is dependent not only on RH but also on the chemical and optical properties of aerosols. The latter dependence may be determined using measurements at fixed two specific humidity levels such as f(85%).

[11] Aerosol extinction, the sum of scattering and absorption, is given as:

$$k_{ext}^a(RH) = k_{sca}^a(RH) + k_{abs}^a. \qquad (3)$$

Since the humidity dependence of aerosol absorption is generally assumed to be negligible [Andrews et al., 2004], no attempt to correct for the humidity effect on the absorption is made in this study. The nephelometers aboard the IAP aircraft measure only submicron-sized (i.e., $D_p <$ 1.0 μm) aerosols. However, supermicron-sized aerosols sometimes become important, so that a correction for supermicron aerosols is necessary. In order to make $f(RH)$ from the IAP data applicable to general ground- and space-based remote sensing instruments, the method proposed by Andrews et al. [2004] is adopted for this correction. In addition, surface measurements made by the Aerosol Observing System (AOS) at the SGP CF are employed, which have similar instrumentation [Sheridan et al., 2001] as the IAP aircraft on-board instruments. In brief, the IAP scattering (and absorption) coefficients for $D_p < 1$ μm were adjusted to represent those for $D_p < 10$ μm by taking the ratios between scattering (and absorption) coefficients for $D_p < 1$ μm and $D_p < 10$ μm from the AOS operating at the surface. This adjustment, for instance, helps bring the IAP measured AOT into agreement with those retrieved from Aerosol Robotic Network (AERONET [Holben et al., 1998]), while it only induces small difference in $f(RH)$.

[12] To infer AOT from the IAP aircraft measurements, the profiles of aerosol extinction coefficients are integrated using a simple trapezoidal scheme. One of the important problems in calculating AOT by integrating aircraft measurements is that aerosols tend to populate at low levels. Andrews et al. [2004] showed a good agreement between the measurements at the lowest flight level and surface measurements. However, such agreement should vary with meteorological conditions and aerosol episodes. So it is possible that the IAP measurements at the lowest flight level do not represent the real aerosols below the level down to the surface. Therefore we combined measurements from the AOS at the surface with the IAP measurements for the AOT calculation.

[13] Scattering coefficients at three different humidity conditions (RH = 40%, RH = 85%, and ambient RH) were computed before and after the correction for supermicron aerosol. We define scattering AOT at different RH levels [$\tau_{sca}(40\%)$, $\tau_{sca}(85\%)$, and $\tau_{sca}(RH)$] as follows:

$$\tau_{sca}(40\%) = \int_{z_1}^{z_2} k_{sca}^a(40\%, z)dz, \qquad (4)$$

$$\tau_{sca}(85\%) = \int_{z_1}^{z_2} k_{sca}^a(85\%, z)dz, \qquad (5)$$

$$\tau_{sca}(RH) = \int_{z_1}^{z_2} k_{sca}^a(RH, z)dz, \qquad (6)$$

where z_1 is the altitude of the surface measurement and z_2 is the highest altitude at which the IAP measurements were made. Likewise, the extinction AOT, $\tau_{ext}(RH)$ can be calculated by integrating the extinction coefficient [equation (3)] in the same manner.

[14] RH values representing the column of interest are necessary in order to relate RH to the derived AOT, so we define a column-mean RH as:

$$\langle wRH \rangle \equiv \int_{z_1}^{z_2} k_{ext}^a(RH, z) \cdot RH(z)dz / \int_{z_1}^{z_2} k_{ext}^a(RH, z)dz, \qquad (7)$$

which is an aerosol extinction weighted column-mean RH, $\langle wRH \rangle$. An arithmetic column-mean RH, $\langle RH \rangle$, which can be defined as:

$$\langle RH \rangle \equiv \int_{z_1}^{z_2} RH(z)dz / \int_{z_1}^{z_2} dz, \qquad (8)$$

might be used when an aerosol extinction profile is unavailable in order to see if there is any statistical relationship with AHE. Alternatively, an average profile of aerosol extinction coefficients [$k_{ext}^{avg}(RH)$] may be used in computing $\langle wRH \rangle$ instead of $k_{ext}^a(RH)$ in equation (7).

[15] The column AHF, $R(RH)$, is defined as the ratio of two AOTs due to scattering at different RH levels:

$$R(RH) \equiv \tau_{sca}(RH)/\tau_{sca}(40\%), \qquad (9)$$

where RH denotes column-mean RH. Likewise, the column AHF can be defined at two fixed RH levels:

$$R(85\%) \equiv \tau_{sca}(85\%)/\tau_{sca}(40\%). \qquad (10)$$

[16] Finally, the relative AHE is defined as:

$$AHE \equiv \frac{\tau_{sca}(RH) - \tau_{sca}(40\%)}{\tau_{ext}(RH)}. \qquad (11)$$

3. Effects of Aerosol Humidification on AOT

[17] To gain a general idea of the AHE, Figure 1 presents the profiles of mean aerosol scattering and extinction profiles and average $f(RH)$ and $f(85\%)$ profiles derived from 70 IAP measurements over the ARM SGP region from April 2003 to June 2004. The aerosol scattering coefficients profiles are provided for three different RH values (i.e., 40%, 85% and ambient), and the aerosol extinction profile at ambient RH is also shown together with the mean ambient RH profile. To show the variability of the profiles for aerosols and their hygroscopicity, statistics (i.e., 5th, 25th, 50th, 75th, and 95th percentiles) for aerosol scattering coefficients at ambient RH and $f(85\%)$ are provided as box-whisker plots. Two different averaging methods were applied to derive $f(RH)$ and $f(85\%)$ profiles as follows: arithmetic averaging and aerosol extinction (at RH = 40%) weighted averaging. The arithmetic mean $f(RH)$ showed small values and decreased slightly with altitude. It is interesting to note that weighted mean $f(RH)$ is larger
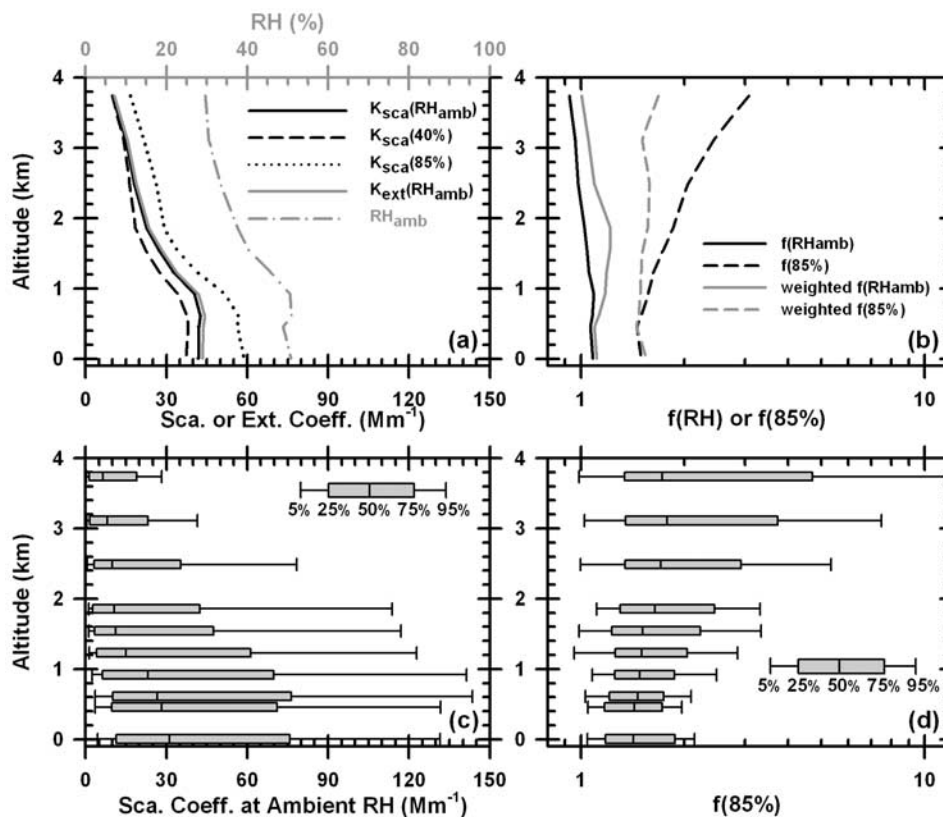
Figure 1. (a) Profiles of aerosol scattering and extinction coefficients (denoted as K_{sca} and K_{ext}), and ambient RH (RHamb) averaged from the IAP measurements (April 2003 to June 2004) at ambient and fixed RH values. (b) Profiles of average f(RH) and f(85%) derived from the IAP measurements. Both the arithmetic and the aerosol extinction weighted averages are provided. (c) Statistics showing 5th, 25th, 50th, 75th, and 95th percentiles of the aerosol scattering coefficients at ambient RH. (d) Statistics (5th, 25th, 50th, 75th, and 95th percentiles) of f(85%).

than arithmetic mean f(RH) in all altitudes especially around 1.5–2 km. It indicates that ambient RH and aerosol extinction for RH = 40% are positively correlated with stronger correlation around 1.5–2-km altitude. On the other hand, arithmetic mean f(85%) increases with altitude and larger than weighted f(85%) above 0.5 km, while weighted f(85%) remained relatively constant around 1.55. This feature is associated with a tendency that increases in aerosol extinction often are accompanied by decreases in f(85%) from the IAP data. It is not clear what caused this feature from the data we have. Two conjectures may be formed, (1) an increase in aerosol extinction at higher altitudes caused by increasing population of hydrophobic aerosols such as smoke or dust, and (2) a bias in the scattering measurements at higher altitudes where scattering coefficients are usually small. The former conjecture may be backed up by some reports on the transported smoke from Siberian fires [*Damoah et al.*, 2004; *Jaffe et al.*, 2004; *Ferrare et al.*, 2006a]. On the other hand, we find most of high f(85%) values are acquired from small scattering coefficient values, which supports the latter. The high variability of f(85%) in the high altitudes (Figure 1d) may happen for both cases; thus further investigation including measurements of aerosol composition will be necessary to understand this feature.

[18] Before dealing with column-mean AHE derived from the IAP data, it is necessary to compare column-total AOT data from different sources. Here we compare the AOT derived from the IAP measurements (hereinafter referred to as IAP AOT) with the AERONET AOT at the time of the IAP measurements. Since IAP observations take ~80 min for a complete nine-level flight [*Andrews et al.*, 2004] and the AERONET measurements would have maximum four to five measurements an hour depending on sky conditions, we allow a 60-min window to match up IAP AOT with the AERONET AOT. Although we fill the gap below the lowest flight level-leg with the AOS measurements, aerosols above the highest flight level-leg were missed. However, roughly 90% of the aerosols over the SGP site tend to reside below 4 km [*Turner et al.*, 2001]. We attempted to correct for the missing aerosols above 4 km using Raman Lidar (RL) measurements of aerosol extinction profiles, proposed by *Andrews et al.* [2004], in order to make the data comparable with the AERONET AOT. Given the ubiquitous small values of AOTs (the minimum and the median of the IAP AOT are 0.021 and 0.090, respectively), an attempt to incorporate stratospheric AOT was made using the monthly mean stratospheric AOT from Stratospheric Aerosol and Gas Experiment (SAGE) II data (version 6.2 available at http://www-sage2.larc.nasa.gov/data/
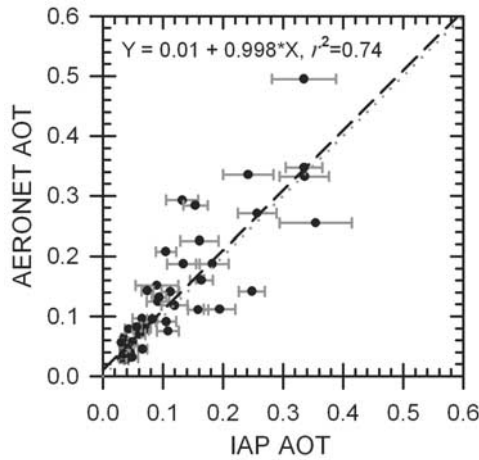
Figure 2. Comparison of AOT derived from IAP flights against AOT measurements from the AERONET. Gray dotted and black dashed lines represent one-to-one and linear fit lines, respectively. Error bars stand for estimated error in the IAP AOT, which is computed by integrating the $\pm 1\sigma$ of the scattering and absorption coefficients in each level-leg.

v6_data/) for a latitude band of $25-45$ degrees north. The IAP-based AOT after all corrections are applied, $\tau_{\text{corr}}^{\text{IAP}}(\text{RH})$, is calculated by

$$\tau_{\text{corr}}^{\text{IAP}}(\text{RH}) = \left(\tau_{\text{sca}}^{\text{IAP}}(\text{RH})/\gamma_{\text{sca}}(\text{RH}) + \tau_{\text{abs}}^{\text{IAP}}/\gamma_{\text{abs}}\right) \\ /(1 - \gamma_{\text{miss}}) + \tau_{\text{strato}}^{\text{SAGE}}, \tag{12}$$

where $\tau_{\text{sca}}^{\text{IAP}}(\text{RH})$, $\tau_{\text{abs}}^{\text{IAP}}$, and $\tau_{\text{strato}}^{\text{SAGE}}$ are scattering AOT at ambient RH and absorption AOT at RH = 40% from the IAP measurements, and stratospheric AOT from SAGE II, respectively, while γ_{sca} and γ_{abs} are correction factors for supermicron aerosols derived from the AOS observations as described in the previous subsection, γ_{miss} is the ratio of RL AOT above the highest IAP level-leg to total RL AOT (used as a proxy for the missing aerosols from the IAP flights). The average values of the correction factors, $\gamma_{\text{sca}}(\text{RH})$, γ_{abs}, and γ_{miss} were 0.83($\pm$0.07), 0.85($\pm$0.09), 0.12($\pm$0.08), respectively.

[19] Figure 2 shows the comparison of γ_{sca} with the AERONET AOT. The AERONET AOT at 500 nm was

adjusted to the value at 550 nm by interpolating the AERONET AOTs at 500 nm and 670 nm. The error bars for the IAP AOT were calculated by integrating ± 1 standard deviation of aerosol scattering and absorption coefficients in each Cessna level-leg. $\tau_{\text{corr}}^{\text{IAP}}(\text{RH})$ is reasonably correlated with the AERONET AOT ($r^2 = 0.74$) with an intercept of 0.01 and a slope of 0.998. This result shows a slight improvement over a comparison made by *Andrews et al.* [2004, intercept = 0.04, slope = 1.04], although the analysis periods are different. Also, their analyses do not include IAP measurements of aerosol scattering at high RH levels. Therefore a humidity correction factor had to be estimated from the surface humidity measurements while the humidity correction is directly determined from the measured data in our study. In addition, the inclusion of the AOS data together with some minor corrections (for example, stratospheric AOT) contributed to this comparison result.

[20] $R(\text{RH})$ and $R(85\%)$ as defined in equations (9) and (10), respectively, were plotted as a function of time in Figure 3. It reveals that $R(\text{RH})$ values during the observation period were very small (mean = 1.09) with little variability (STD = 0.12), indicating that the contribution of the AHE to the total AOT is small on average. On the other hand, $R(85\%)$ is significantly larger (1.55 $\pm$ 0.30) than
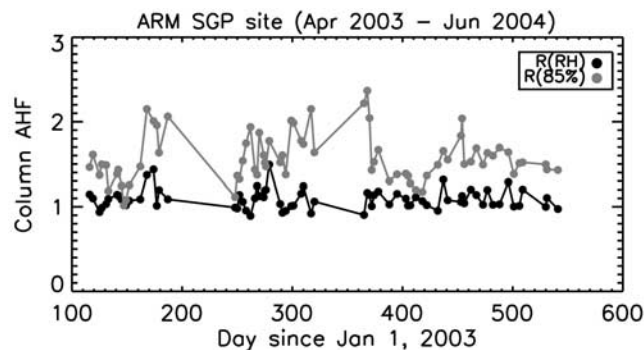

Figure 3. Time series of the column AHF derived from IAP observations. Black line stands for column AHF for the ambient RH profiles, or $R(\text{RH})$, while gray line corresponding to a fixed RH = 85%, or $R(85\%)$.
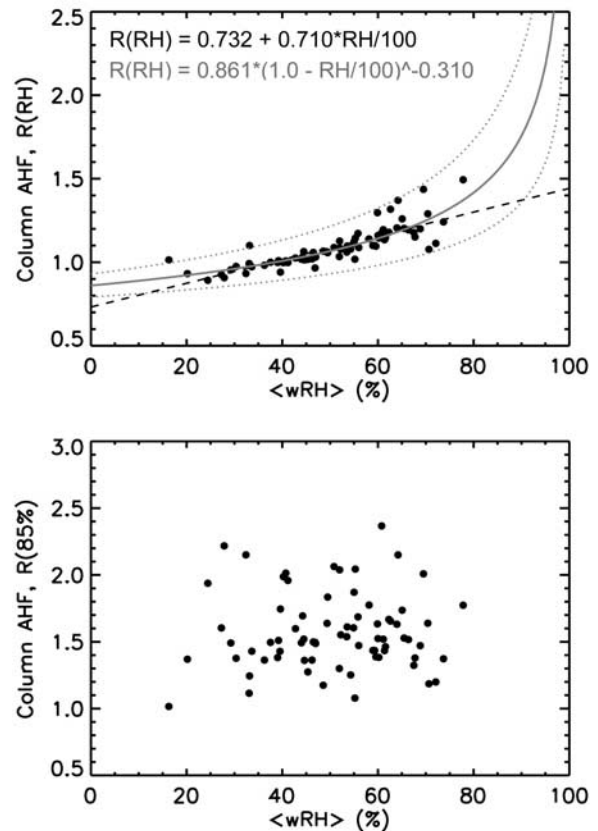

Figure 4. Column-mean AHF, $R(\text{RH})$ as a function of column-mean RH weighted by aerosol extinction (upper panel). Linear (black dashed line) and two-parameter fitting (gray solid line) lines are provided. Gray dotted lines corresponds to $\pm 2\sigma$ of fitted parameters, providing range of uncertainty. Column-mean $R(85\%)$ is plotted against column-mean RH in the lower panel.
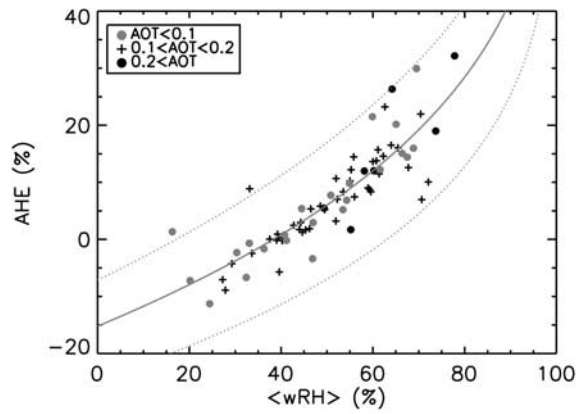
Figure 5. Relative AHE (percentage to the total AOT) as a function of the column-mean RH. Data points of different ranges of AOT values are shown in different symbols. The solid line is the regressional fitting, and the dotted line is the estimated range of uncertainty (i.e., $\pm 2\sigma$ of fitted parameters).

$R(\text{RH})$, implying that there were significant potentials of AHE, but the atmospheric conditions observed by IAP aircraft over the SGP were rather dry. When the data shown in Figure 3 are plotted as a function of $\langle \text{wRH} \rangle$, which is

derived using aerosol extinction and ambient RH profiles from the IAP measurements, AHE can be viewed clearly (Figure 4). $R(\text{RH})$, shown in the upper panel, illustrates a clear dependence on $\langle \text{wRH} \rangle$ and is reasonably fitted to both linear and nonlinear curves. The nonlinear curve generally provides a better fit for higher RH values, but the uncertainty may also be larger, especially when $\langle \text{wRH} \rangle$ is greater than 80%. However, since $\langle \text{wRH} \rangle$ is a column quantity, such high $\langle \text{wRH} \rangle$ is very rare in the real atmosphere. Contrary to $R(\text{RH})$, the column AHF at a fixed RH level, $R(85\%)$, shows no dependence on $\langle \text{wRH} \rangle$. $R(85\%)$ pertains information about aerosol chemical/optical properties and correlation between aerosol extinction and RH but not necessarily pertinent to the absolute magnitude of RH.

[21] On the basis of the above discussions, the AHE for the total (i.e., scattering + absorption) AOT is plotted as a function of the aerosol extinction weighted column-mean RH, $\langle \text{wRH} \rangle$, in Figure 5. Although some theoretical studies suggested possible dependence of aerosol absorption for mixture of certain types of aerosols [e.g., *Lesins et al.*, 2002], there is no information available yet concerning the dependence of aerosol absorption on RH over the SGP site; thus it is assumed that the AHE influences only on the aerosol scattering. The AHE is defined as the ratio of the difference
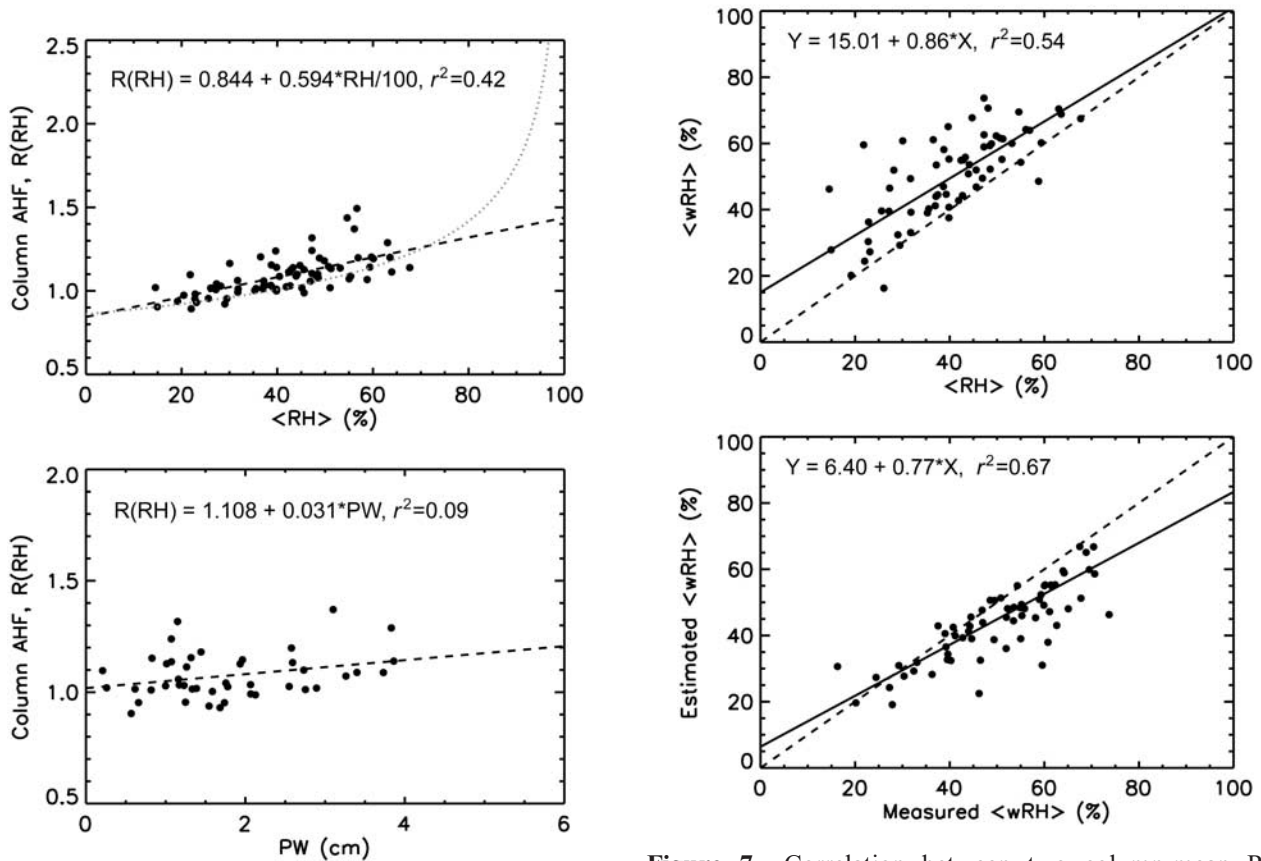

Figure 6. Similar to Figure 4 but as functions of simple arithmetic means of RH ($\langle \text{RH} \rangle$; upper panel) and precipitable water (PW; lower panel). The dashed lines are least squared linear regressions. A gray dotted line in the upper panels is the same as the gray solid line shown in Figure 4 and provided here for a reference.

Figure 7. Correlation between two column-mean RH obtained by simple arithmetic averaging of RH ($\langle \text{RH} \rangle$.) and weighted by the aerosol extinction coefficient ($\langle \text{wRH} \rangle$) (upper panel). Comparison of measured $\langle \text{wRH} \rangle$ with estimated $\langle \text{wRH} \rangle$ using measured RH profiles and an average aerosol extinction profile (lower panel). Solid and dashed lines represent linear fit and one-to-one lines, respectively.

Table 2. Proposed Methods of Estimating the Relative Humidity Effect on the Aerosol Optical Thickness When Direct Measurements are Not Available

Method ID	Description	Required Inputs	Assumptions
M1	Uses equation (13) and $\langle wRH \rangle$ calculated from measurement	Profiles of ambient RH and aerosol extinction at ambient RH	Empirical relationship between column RH and R(RH)
M2	Uses equation (13), but $\langle wRH \rangle$ is estimated from a linear relationship, $\langle wRH \rangle = c + d\langle RH \rangle$, where $c = 15$, $d = 0.86$	Ambient RH profile (or column-mean RH)	Empirical relationships between column RH and R(RH) and between $\langle wRH \rangle$ and $\langle RH \rangle$
M3	Uses equation (13), but $\langle wRH \rangle$ is estimated from an average profile of aerosol extinction at ambient RH [i.e., $k_{ext}^{avg}(RH)^a$] and measured RH profiles, i.e., $\langle wRH \rangle = \dfrac{\int k_{ext}^{avg}(RH, z)RH(z)dz}{\int k_{ext}^{avg}(RH, z)dz}$	Ambient RH profile and mean (or assumed) aerosol extinction profile	Empirical relationship between column RH and R(RH); profile of aerosol extinction
M4	Uses equation (14) from average profiles[a] of aerosol scattering coefficient at RH = 40% [i.e., $k_{sca}^{avg}(40\%)$], and $f(85\%)$ [i.e., $f^{avg}(85\%)$] and measured RH profiles	Profiles of ambient RH, mean (or assumed) aerosol scattering coefficient at RH $\leq$ 40%, and mean (or assumed) f(RH)	Profiles of aerosol scattering at RH = 40% and $f(85\%)$
M5	Uses $k_{sca}^{avg}(40\%)$ and measured RH profiles; set the profile of $f(85\%)$ to a constant whose value is the same as the one observed at a surface station [i.e., $f_{sfc}^{AOS}(85\%)^b$]	f(RH) measured at the surface and profiles of ambient RH, mean (or assumed) aerosol scattering coefficient at RH $\leq$ 40%	Profiles of the aerosol scattering at RH = 40%, and $f(85\%)$
M6	Uses measured profiles of $k_{sca}^{avg}(40\%)$ and RH; set $f(85\%) = f_{sfc}^{AOS}(85\%)$	f(RH) measured at the surface and profiles of ambient RH, aerosol scattering coefficient at RH $\leq$ 40%	Profile of $f(85\%)$

[a]Average profiles of aerosol scattering, extinction, f(RH), and $f(85\%)$) are provided in Figure 1.
[b]f_{sfc}^{AOS} denotes $f(85\%)$ measured from the Aerosol Observing System [*Sheridan et al.*, 2001] at the surface of the ARM SGP CART site.

between the scattering AOT derived for the ambient RH profiles and the scattering AOT at RH = 40% to the extinction AOT with ambient RH profiles [see equation (11)]. Data points with different AOT ranges are presented in different colors and symbols to see if any dependence of the AHE on the magnitude of AOT is evident. The AHE, of which values range from −6 to 25%, shows an exponential dependence on $\langle wRH \rangle$. *Öström and Noone* [2000] reported that humidity-induced growth of aerosols over oceans could contribute about more than half of the measured AOT. The AHE over the SGP appears lower than the results by *Öström and Noone* [2000], which possibly results from drier atmospheric conditions over the SGP site and differences in the size of dry aerosol particles and their chemical composition. However, we cannot rule out the possibility of more hydrophobic aerosols present over the SGP site. Some researches have reported smoke aerosols transported over the SGP site [e.g., *Damoah et al.*, 2004; *Jaffe et al.*, 2004; *Wang et al.*, 2006].

4. Estimating the Column Aerosol Humidification Factor

[22] If aerosol profiles are not available (often the case), R(RH) might be determined by arithmetic column-mean RH or precipitable water (PW) alone, as RH profiles or PW are more readily available than aerosol profiles. Figure 6 shows the relationships between R(RH) and $\langle RH \rangle$ and PW. Although these relationships show weaker correlations than that of the one using $\langle wRH \rangle$, linear relationships do exist. There are fewer data points for R(RH) versus PW plot because of less match-ups for PW, which is obtained from the AERONET measurements. The linear relationships may be used to estimate R(RH) for a limited range of column-mean RH (for example, 20–70%). However, given the

nonlinear response of AHE to RH, R(RH) tends to be underestimated for higher RH.

[23] When only RH profile measurements are available, two different approaches may be adopted to estimate R(RH), (1) using $\langle RH \rangle$ in lieu of $\langle wRH \rangle$ and (2) using an average aerosol extinction coefficient profile as a priori. $\langle RH \rangle$ is correlated with $\langle wRH \rangle$ reasonably well ($r^2 = 0.53$), as shown in the upper panel of Figure 7. In general, $\langle wRH \rangle$ is higher than $\langle RH \rangle$ indicating that aerosol extinction profiles are positively correlated with RH profiles. These two column-mean RH values approach each other as RH increases. In the lower panel of Figure 7, $\langle wRH \rangle$ estimated using an average aerosol extinction profile (presented in Figure 1) instead of the observed aerosol extinction profiles was compared against the measured $\langle wRH \rangle$. The estimated $\langle wRH \rangle$ has a better correlation with the measured $\langle wRH \rangle$ than $\langle RH \rangle$ but tends to be lower. Thus it is better to use an average aerosol extinction profile to estimate $\langle wRH \rangle$.

[24] Six methods (hereinafter, denoted as M1−M6) to estimate R(RH) are introduced in Table 2. In brief, M1−M3 utilize the relationship between $\langle wRH \rangle$ and R(RH) as shown in Figure 4. The R(RH) values are derived using the column-mean RH of aerosol extinction (i.e., $\langle wRH \rangle$) similar to equation (2):

$$R(\text{RH}) = a \cdot \left(1 - \frac{\langle wRH \rangle}{100}\right)^{-b}, \quad (13)$$

where $a = 0.861$ and $b = 0.310$ that were derived in Figure 4. M1~M3 differ in ways for deriving $\langle wRH \rangle$. M1 can be applied when both aerosol extinction and RH profiles are available. M2 uses a known a priori relationship between $\langle RH \rangle$ and $\langle wRH \rangle$, so that $\langle wRH \rangle$ may be estimated without aerosol profiles. In M3, $\langle wRH \rangle$ is estimated from an average profile of aerosol extinction. In the methods M4~M6, R(RH)
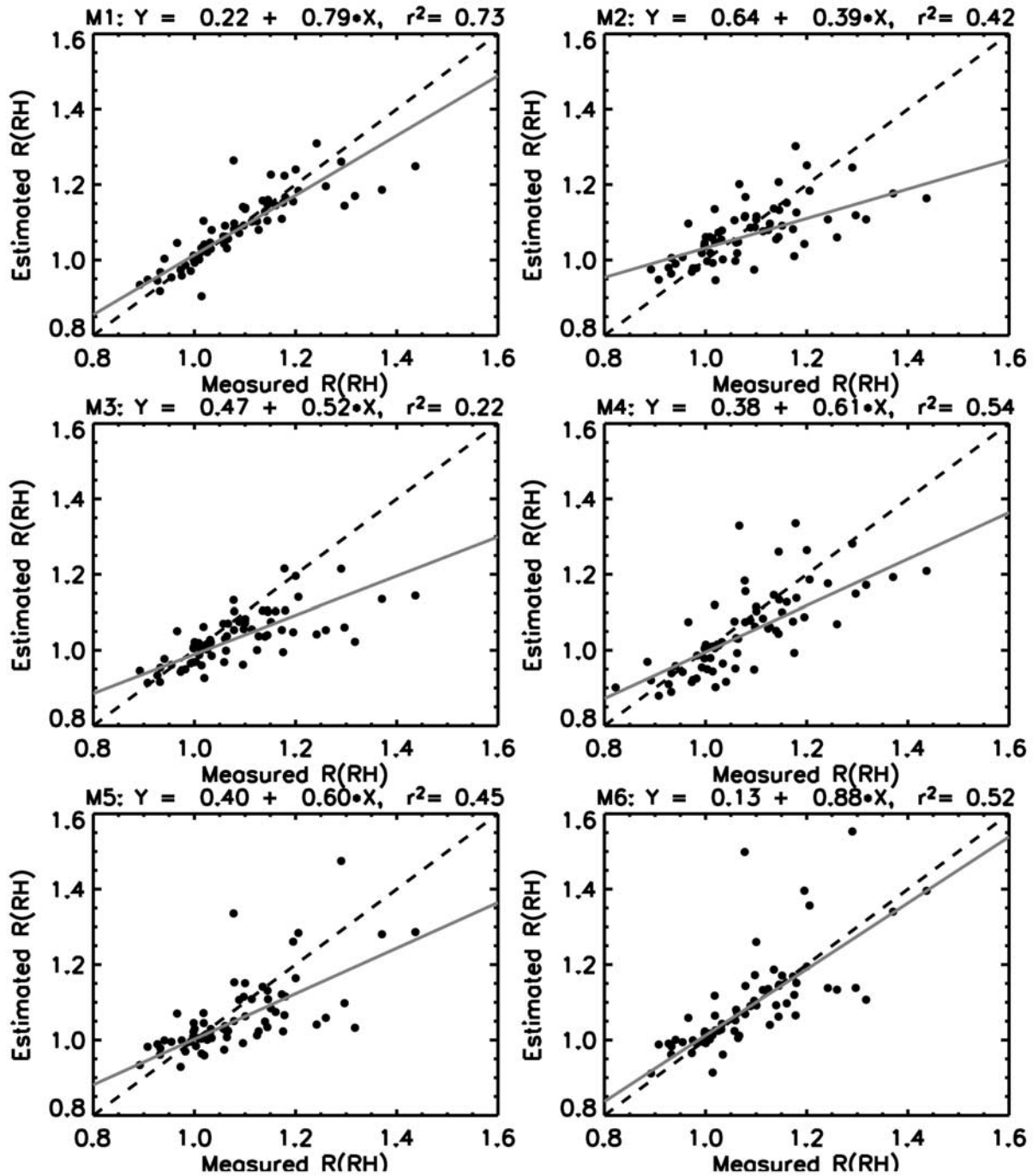
Figure 8. Comparison of estimated column AHF, R(RH) following six different methods (M1∼M6). Gray solid lines and black dashed lines are linear fit and one-to-one lines, respectively.

was computed by directly integrating the assumed aerosol profiles. M4 and M5 use

$$R(\text{RH}) = \frac{\int k_{\text{sca}}^{\text{avg}}(40\%, z) f^{\text{est}}(\text{RH}) dz}{\int k_{\text{sca}}^{\text{avg}}(40\%, z) dz}, \tag{14}$$

where $k_{\text{sca}}^{\text{avg}}(40\%)$ is the average aerosol scattering profile at RH = 40%, and f^{est}(RH) is a profile of the aerosol scattering humidification factor estimated from a measured RH profile with an assumed f(85%) profile. When f(85%) can be estimated, f(RH) may be calculated by combining equations (1) and (2). M4 uses an average profile of f(85%) while M5 uses a measurement of f(85%) at the surface assuming the same f(85%) value aloft. For M6, R(RH) can be derived by replacing $k_{\text{sca}}^{\text{avg}}$ with an observed k_{sca} (∼40%) in equation (14). M6 has been suggested to use if f(85%) or b in equation (2) can be assumed when the profiles of aerosol scattering
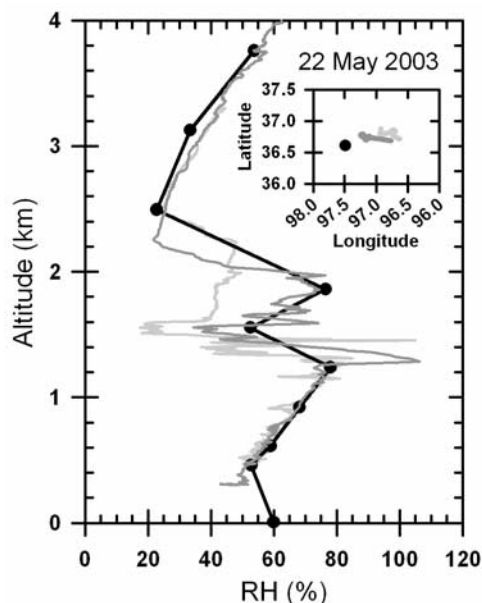
Figure 9. A profile of RH obtained from an IAP flight and a coincident AOS measurement at the surface (solid black line; measured for 16:20–17:46Z) and two profiles of ambient RH from Twin Otter flights during the Aerosol Intensive Operation Periods over the SGP site in 2003 (dark and bright gray lines; measured for 16:46–17:15Z and 17:51–18:15Z, respectively). The locations of measurements are also indicated in the subpanel.

coefficients at a low-humidity condition (RH ~40%) are measured [e.g., *Remer et al.*, 1997; *Andrews et al.*, 2004].

[25] The estimated R(RH) using the proposed methods (M1–M6) are compared with the measured R(RH) in Figure 8. Linear regression coefficients and r^2 are provided in the figure, and the root mean squared errors for M1–M6 are 0.059, 0.086, 0.094, 0.086, 0.090, and 0.091, respectively. Among the methods, M1 shows the best agreement followed by M6, which is not a surprise since equation (13) is derived by fitting to the measured R(RH). M6 has been used in the literature [e.g., *Remer et al.*, 1997; *Andrews et al.*, 2004]. The two methods are applicable to different situations. For example, M1 can be applied to RL measurements from which profiles of aerosol extinction coefficients at ambient RH are available together with RH [e.g., *Turner et al.*, 2001]. On the other hand, M6 can be used when airborne measurements of aerosol scattering coefficients are obtained only at a low-humidity RH condition [e.g., *Andrews et al.*, 2004]. The overall results in Figure 8 can be summarized as follows: (1) when both aerosol extinction and RH profiles are available, best estimation of R(RH) is achieved using M1, followed by M6; (2) when aerosol profiles are unavailable, use of representative profiles of aerosol scattering coefficients and f(85%) (i.e., M4) would be a next choice, followed by M5, which uses f(85%) measured at the surface. It should be noted, however, that all the methods tend to underestimate R(RH). Such R(RH) underestimation for M2~M5 originates from the fact that aerosol profiles tend to be correlated to RH in natural conditions, which was not necessarily the case when an average aerosol profile was used. Also, the limited range of $\langle$wRH$\rangle$

used in M1–M3 to derive equation (13) degrades the R(RH) estimation at higher RH, i.e., $\langle$wRH$\rangle$ greater than 80%.

5. Sensitivity of the Column Aerosol Humidification Factor to a Very Humid Layer

[26] We have tested the sensitivity of R(RH) to the presence of a very humid layer, which could be missed by the IAP observations. This scenario may happen when there is a layer of scattered clouds or a locally very humid layer, which is distant from where an IAP observation was made. Figure 9 shows such an example. The figure shows a RH profile obtained from an IAP flight at discrete levels and a ground RH from the Temperature, Humidity, Wind, And Pressure Systems at the ARM SGP CF site. Besides, two continuous RH profiles were acquired from the Twin Otter aircraft during the aerosol intensive observation period over the SGP site in 2003 [*Ferrare et al.*, 2006b]. The IAP RH profile agrees very well with the other two RH profiles taken from Twin Otter at slightly different locations and times, except for sharp peaks (RH > 100%) with a thickness of 0.1–0.2 km, illustrating the presence of very humid layer missed by the IAP data. Thus it is assumed there is a humid layer with RH = 99% that the IAP measurements missed among the nine-level legs plus a layer between the surface and the lowest level-leg per flight. The altitudes of the respective level-legs are provided in Table 1. In each test, the observed ambient RH for a selected level-leg was replaced by RH = 99%. This test was repeated for the ten levels, respectively. The scattering coefficient for the selected layer (that is, the layer where RH was forced to be 99%) was recalculated to derive the AOT. A series of such sensitivity tests were performed for cases when a very humid layer exists in the different altitudes. Figure 10 shows R(RH) as a function of $\langle$wRH$\rangle$, derived from the sensitivity test with very humid layer thickness equal to the thickness of the IAP level-legs. The observed R(RH) without consideration of the humid layer was also provided for reference. For example, R(RH) values for an atmospheric column containing a very humid layer with a thickness of the IAP level-leg centered at 3.1 km can be as high as 5 while the maximum of the observed R(RH) was 1.3. The more sensitivities of R(RH) occur, the higher the altitudes of a humid layer. This may result from the fact that the thickness of IAP level-legs are larger for higher altitudes. On the other hand, if atmospheric layers at higher altitudes (>3 km) are normally drier than those at lower altitudes, it can cause higher sensitivity at higher altitudes. However, if aerosol extinction is too low, the effect is small, just as shown for the highest level-leg (3.6 km). The dashed line in Figure 10 was derived by fitting all the data shown in the figure to equation (13). The coefficients a and b for this the curve are 0.728 and 0.621, respectively.

[27] It is necessary to normalize R(RH) to those values found when there are equal thicknesses of the humid layer at different levels in order to see if there is any dependence of R(RH) on the altitudes of the humid layer. Thus similar sensitivity tests as those made previously were performed but with a fixed thickness (Δz = 0.2 km) of the very humid layers. Figure 11 depicts that high R(RH) values (>3.0) shown in the previous tests (Figure 10) vanished, suggesting that the larger very humid layer thicknesses are the primary
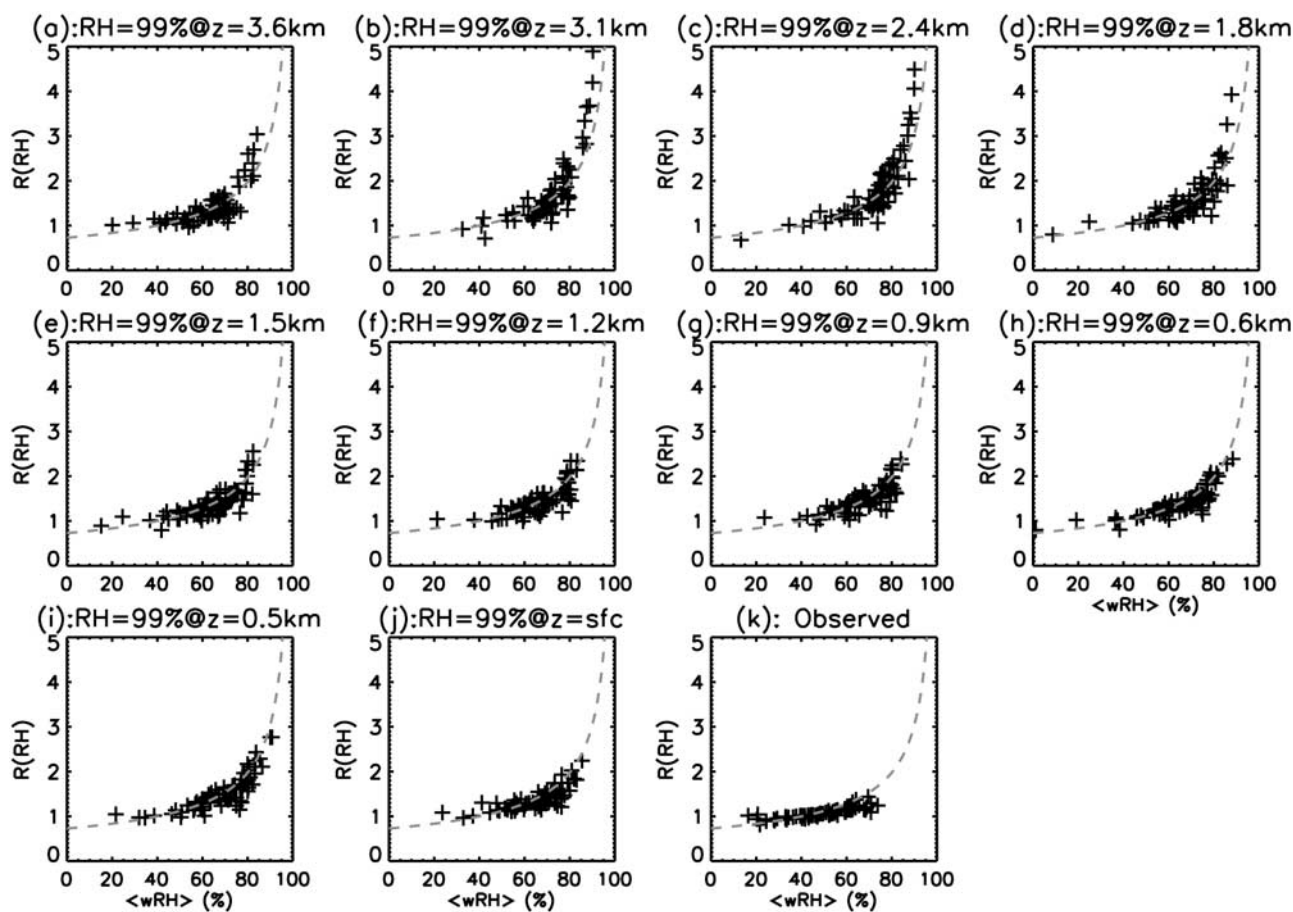
Figure 10. (a–j) Column-mean AHF as functions of the weighted column-mean RH, $\langle$wRH$\rangle$. The ambient RH at 1 of the 10 level-legs of the IAP measurements is replaced with RH = 99%. The bottom of the replaced layer is indicated in each panel (a–j), where the aerosol scattering coefficients and AOT were recalculated accordingly. (k) The same as (a–j) but using the original ambient RH profile. The gray dashed line is the fitting line of equation (13) to the all the data shown in this figure.

reason for high R(RH) sensitivity at high altitudes. Also, the value of R(RH) is normally less than 2 and does not depend on the altitude of the humid layer when Δz is fixed. These results show that a "missing" humid layer could introduce slight discrepancies of R(RH) from what was observed from the IAP flights, when a reasonable thickness of such layer is considered. The AOT due to aerosol scattering within a very humid layer was compared with that with the observed ambient RH profiles in Figure 12. The AOT due to aerosol scattering within the humid layer is systematically higher than the observed. Such systematic differences (0–20%) vary with the altitude of the humid layer with a tendency of larger systematic differences for the cases when the humid layers exist at low levels in the atmosphere. This result seems reasonable because the aerosol population is normally larger at low levels (for example, <2 km).

[28] Additional tests on the sensitivity of R(RH) to the thickness of the assumed humid layer were conducted with different thickness (Δz) values of the humid layer. The results are summarized in Tables 3 and 4 for cases with $\Delta z = 0.1$ km, $\Delta z = 0.2$ km, $\Delta z = 0.3$ km, and Δz equal to the thickness between the IAP flight level-legs. No significant dependence on the altitude of the very humid layer was found except for the highest level (3.6 km),

which showed a smaller sensitivity than the other levels. It is mainly because of the small population of aerosols at that (and above) altitude. The average R(RH) for all the IAP data available in this study (i.e., 70 profiles) was 1.09 ± 0.12. In Table 3, R(RH) changes 4~13% from the observed R(RH) when $\Delta z = 0.1$ km, and varies 9~27% and 15~42% when $\Delta z = 0.2$ km and $\Delta z = 0.3$ km, respectively. These R(RH) changes result in AOT changes from the observed by up to 9, 19, and 28% for the respective Δz. These values, in turn, correspond to the AHE on AOT by 15~25, 15~41, and 15~55% for the respective Δz, as given in Table 3.

6. Summary and Suggestion

[29] The AHE on the AOT measured over the SGP site was investigated. AOTs at different RH levels (for example, RH = 40 and 85% throughout the column, and ambient RH profiles) were computed by integrating aerosol extinction profiles measured from a light aircraft (Cessna C-172N) under the In situ Aerosol Profiles (IAP) project, which is a joint effort between the ARM program of Department of Energy and the Climate Monitoring and Diagnostics Laboratory of the National Oceanic and Atmospheric Adminis-
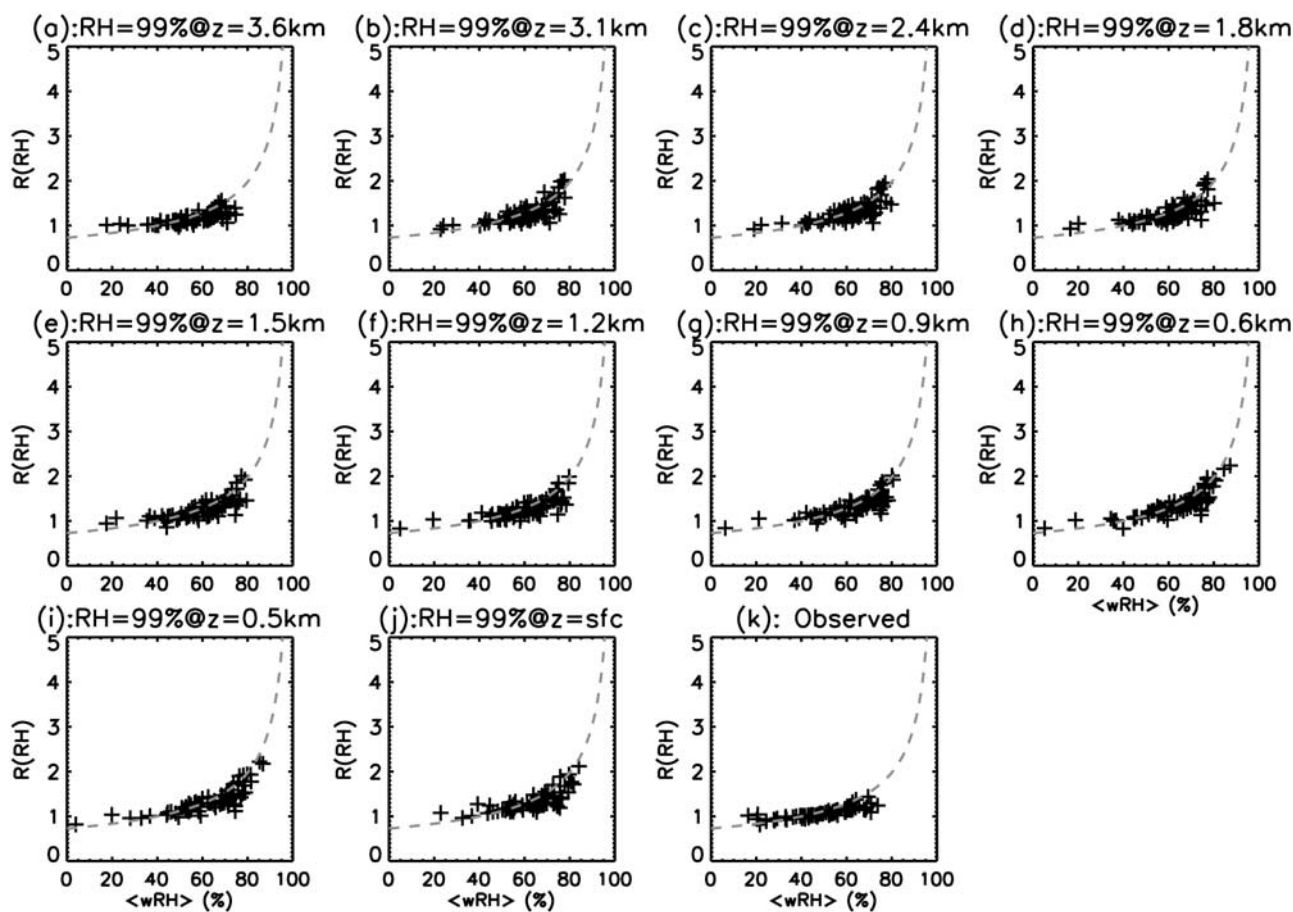
Figure 11. The same as Figure 10, but the thickness of very humid layer (RH = 99%) was set to 0.2 km for respective levels shown in panel (a–j). The dashed gray line is the same line as shown in Figure 10.

tration. The AOT derived from the IAP agreed reasonably well with coincident AOT from the AERONET.

[30] Conventional two-parameter fitting [*Hänel*, 1976] was used to estimate f(RH) at ambient RH and at 85% from the scattering coefficients measured during the IAP flights. This f(RH) was used to compute the aerosol scattering coefficients at different RH values (40%, 85%, and ambient RH). Then, those aerosol scattering coefficients were integrated vertically to derive AOT at different RH values.

[31] The column AHF, R(RH), was defined as the ratio of the AOT with an ambient (or desired) RH profile to the AOT at a 40% RH level throughout the column. R(RH) for ambient RH profiles for all available IAP data barely exceeds 1.3, which suggests that the AHE under the normal conditions of the IAP observations is small [mean R(RH) = 1.09 ± 0.12]. The ambient column-mean RH for the data used in this study spanned 20–80%. An AOT increase in response to column-mean RH increase is less than 30% compared with an AOT measured at a low-humidity level (RH = 40%). On the other hand, the column AHF at RH = 85%, R(85%), was greater than 1.5 for the majority of cases (mean equal to 1.57 ± 0.28), implying that the R(RH) could have been larger than the observed if the column-mean RH were higher or profiles of aerosols and RH were correlated better. It was shown that R(RH) can be represented as increasing functions of humidity variables such as the

arithmetic column-mean RH ($\langle$RH$\rangle$), PW, and aerosol extinction weighted column-mean RH ($\langle$wRH$\rangle$).

[32] Six methods to estimate R(RH) are introduced and compared with measured R(RH). These alternative methods may be useful when direct measurements of R(RH) are not available. The results suggest that the relationship between $\langle$wRH$\rangle$ and R(RH) works best if the profiles of humidity and aerosol extinction are available. If the data are not available, use of other relationships pending on available measurements may be resorted to with a varying accuracy.

[33] The sensitivity of R(RH) to a very humid layer (RH = 99%) was tested. Since the IAP data used in this study have a coarse vertical resolution (0.2–0.65 km), it is possible for the IAP observations to miss a layer of very high RH at or near the location of the measurements, especially when clouds exist nearby. R(RH) changed approximately 8, 19, and 31% from the observed R(RH) with changes in the thickness of the very humid layer, Δz, (0.1, 0.2, and 0.3 km, respectively). R(RH) is insensitive to the altitude of the humid layer. The variability of R(RH) with different locations of the humid layer was about 2–6%, depending upon the Δz (0.1–0.3 km). Finally, it was estimated that AOT changes up to 9, 19, and 28% from the observed (ambient) AOT as Δz changes by 0.1, 0.2, and 0.3 km, respectively. These AOT changes correspond to an AHE on the AOT (that is, AOT changes from AOT at RH = 40%) of 27, 41, and 55%, respectively. Therefore the AHE on the
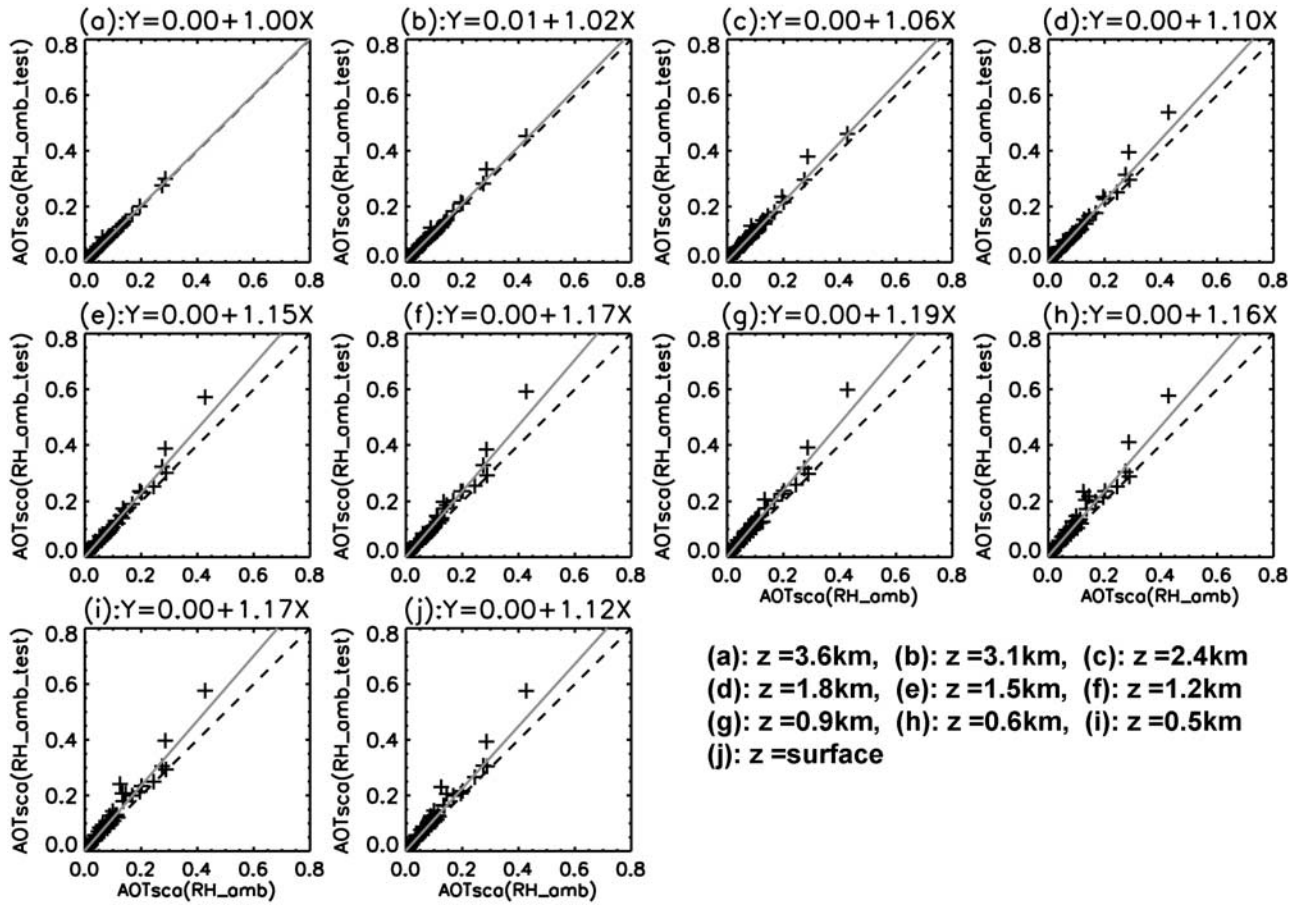
Figure 12. Comparisons between observed AOT and those derived assuming a humid layer of 0.2 km. Dashed black and solid gray line stand for one-to-one and linear fit lines, respectively. Figure 12a–12j correspond to the tests as described in Figure 11.

AOT over the SGP site is not likely to exceed 50% on average compared with the AOT at low-humidity conditions (RH = 40%).

[34] The results and methodology presented are useful to estimate the contribution of the AHE on changes in AOT derived from Sun photometers or from satellite-based retrievals. There have been attempts to use AOT to study the AIEs [e.g., *Nakajima et al.*, 2001; *Bréon et al.*, 2002; *Koren et al.*, 2005; *Kaufman et al.*, 2005b] with an implicit assumption that AOT is a proxy of aerosol loading and CCN. If the AHE contributes substantially to changes in AOT, its values obtained after subtracting the contribution

Table 3. Averages of the Column Aerosol Humidification Factor Derived From the Sensitivity Test for the Given Thickness (Δz) of a Very Humid (RH = 99%) Layer[a]

Test ID[b]	Mean R(RH)			
	Δz = level-leg thickness[c]	Δz = 0.1 km	Δz = 0.2 km	Δz = 0.3 km
1	1.420 (±0.415)	1.117 (±0.112)	1.174 (±0.139)	1.235 (±0.194)
2	1.772 (±0.774)	1.174 (±0.139)	1.288 (±0.241)	1.407 (±0.367)
3	1.838 (±0.724)	1.185 (±0.143)	1.308 (±0.235)	1.439 (±0.347)
4	1.573 (±0.527)	1.169 (±0.140)	1.277 (±0.229)	1.392 (±0.339)
5	1.387 (±0.331)	1.163 (±0.149)	1.268 (±0.225)	1.375 (±0.324)
6	1.415 (±0.322)	1.173 (±0.152)	1.288 (±0.225)	1.405 (±0.320)
7	1.495 (±0.330)	1.200 (±0.158)	1.341 (±0.234)	1.486 (±0.330)
8	1.416 (±0.318)	1.216 (±0.182)	1.372 (±0.288)	1.534 (±0.412)
9	1.520 (±0.410)	1.212 (±0.180)	1.363 (±0.286)	1.520 (±0.409)
10	1.364 (±0.239)	1.193 (±0.156)	1.327 (±0.219)	1.466 (±0.300)
Observed	1.090 (±0.116)			

[a]The numbers in the parentheses are standard deviation. (N = 70) N is the total number of the IAP profiles.

[b]Set to equal to the level-leg ID at which observed RH was replaced with RH = 99% assuming a hypothetical humid layer that could have missed by the IAP measurements in the sensitivity test.

[c]Level-leg thickness are approximately 0.5, 0.6, 0.65, 0.45, 0.3, 0.3, 0.3, 0.2, 0.3, and 0.25 km for level IDs from 1 to 10, respectively.

Table 4. The Slope Between the Scattering AOT Including Very Humid Layer (Thickness, Δz) and Scattering AOT at RH = 40%[a]

Test ID	Slope			
	Δz = level-leg thickness	Δz = 0.1 km	Δz = 0.2 km	Δz = 0.3 km
1	1.17	1.15	1.15	1.15
2	1.25	1.17	1.18	1.23
3	1.38	1.18	1.22	1.25
4	1.35	1.20	1.24	1.30
5	1.36	1.22	1.33	1.37
6	1.52	1.27	1.38	1.49
7	1.52	1.25	1.40	1.51
8	1.47	1.25	1.41	1.55
9	1.40	1.25	1.32	1.43
10	1.32	1.23	1.31	1.41
Observed	1.15			

[a]Intercepts for all cases were set to 0.

of AHE would be a better proxy for CCN and thus more valuable for observational studies of the AIE [e.g., *Feingold et al.*, 2003, 2006]. Another application is to help quantify cloud contamination using the AOT retrieved from satellites or measured by automated Sun photometers. Correlation between AOT and cloud fraction has been reported, but it is unclear whether it is caused by cloud contamination or AHEs or both [e.g., *Ignatov and Nalli*, 2002; *Jeong and Li*, 2005; *Kaufman et al.*, 2005a]. After removing the AHE effect, the magnitude of cloud contamination can be better estimated.

Appendix A: Error Analyses on f(RH) and R(RH)

[35] Suppose errors are additive in the measured aerosol scattering coefficients. Considering the errors, f(RH) in equation (1) can be written as

$$f(\mathrm{RH}) + \Delta f(\mathrm{RH}) = \frac{k_{\mathrm{sca}}^a(\mathrm{RH}) + \Delta k_{\mathrm{sca}}^a(\mathrm{RH})}{k_{\mathrm{sca}}^a(40\%) + \Delta k_{\mathrm{sca}}^a(40\%)}, \quad (\mathrm{A1})$$

where $\Delta k_{\mathrm{sca}}^a(40\%)$ and $\Delta k_{\mathrm{sca}}^a(\mathrm{RH})$ are errors in scattering coefficient at RH = 40% and ambient RH, and $\Delta f(\mathrm{RH})$ is an error in f(RH). Equation (A1) reduces to

$$\Delta f(\mathrm{RH}) = \frac{\varepsilon_2 - \varepsilon_1 \cdot f(\mathrm{RH})}{1 + \varepsilon_1}, \quad (\mathrm{A2})$$

where ε_1 and ε_2 are relative error of aerosol scattering coefficient at RH = 40% and ambient RH, which are defined as $\varepsilon_1 \equiv \Delta k_{\mathrm{sca}}^a(40\%) / k_{\mathrm{sca}}^a(40\%)$ and $\varepsilon_2 \equiv \Delta k_{\mathrm{sca}}^a(\mathrm{RH}) / k_{\mathrm{sca}}^a(40\%)$, respectively. An error of R(RH) under presence of additive scattering AOT error is analogous to that of f(RH).

[36] An error in the correction of the IAP AOT for the presence of supermicron aerosol particles can also propagate to an error in R(RH). R(RH) is computed from the IAP AOT as follows:

$$R(\mathrm{RH}) = \frac{\tau_{\mathrm{sca}}^{\mathrm{IAP}}(\mathrm{RH})/\gamma_{\mathrm{sca}}(\mathrm{RH})}{\tau_{\mathrm{sca}}^{\mathrm{IAP}}(40\%)/\gamma_{\mathrm{sca}}(40\%)}. \quad (\mathrm{A3})$$

[37] Suppose there are additive errors in the correction factors; then equation (A3) becomes

$$R(\mathrm{RH}) + \Delta R(\mathrm{RH}) = \frac{\tau_{\mathrm{sca}}^{\mathrm{IAP}}(\mathrm{RH})}{\tau_{\mathrm{sca}}^{\mathrm{IAP}}(40\%)} \frac{\gamma_{\mathrm{sca}}(40\%) + \Delta\gamma_{\mathrm{sca}}(40\%)}{\gamma_{\mathrm{sca}}(\mathrm{RH}) + \Delta\gamma_{\mathrm{sca}}(\mathrm{RH})}, \quad (\mathrm{A4})$$

where $\Delta R(\mathrm{RH})$, $\Delta\gamma_{\mathrm{sca}}(40\%)$, and $\Delta\gamma_{\mathrm{sca}}(\mathrm{RH})$ are errors in R(RH), correction factor at RH = 40% and ambient RH, respectively. Equation (A4) is rewritten as follows:

$$\Delta R(\mathrm{RH}) = R(\mathrm{RH}) \cdot \left(\frac{1 + \varepsilon_1'}{1 + \varepsilon_2'} - 1\right), \quad (\mathrm{A5})$$

where ε_1' and ε_2' are relative errors in $\Delta\gamma_{\mathrm{sca}}(40\%)$ and $\Delta\gamma_{\mathrm{sca}}(RH)$, which are defined as $\varepsilon_1' \equiv \Delta\gamma_{\mathrm{sca}}(40\%) / \gamma_{\mathrm{sca}}(40\%)$ and $\varepsilon_2' \equiv \Delta\gamma_{\mathrm{sca}}(\mathrm{RH}) / \gamma_{\mathrm{sca}}(\mathrm{RH})$, respectively. Note that the relative error [i.e., $\Delta R(\mathrm{RH}) / R(\mathrm{RH})$] is independent of R(RH), different from the case when scattering coefficients (or AOT) pertain additive errors as in equation (A2). We do not have direct measurements of ε_1' and ε_2' for the data used in this study, but the variability (i.e., standard deviation) of $\gamma_{\mathrm{sca}}(\mathrm{RH})$ measured from the AOS at the surface during the period of the study was around 0.07 with average $\gamma_{\mathrm{sca}}(\mathrm{RH})$ around 0.83. Assuming it represents the approximated range of the errors, the magnitudes of ε_1' and ε_2' are around 10% and the corresponding $\Delta R(\mathrm{RH}) / R(\mathrm{RH})$ is less than 20%.

[38] Errors in fitting parameters (i.e., a and b) and $\langle wRH \rangle$ are another source of errors in estimating R(RH) using equation (13). From equation (13) such errors can be described as follows:

$$R(\mathrm{RH}) + \Delta R(\mathrm{RH}) = \frac{1}{R(\mathrm{RH})} \cdot (a + \Delta a)$$
$$\cdot \{1 - (\langle wRH \rangle + \Delta\langle wRH \rangle)\}^{-(b+\Delta b)}, \quad (\mathrm{A6})$$

where Δa, Δb, and $\Delta\langle wRH \rangle$ are the errors in the fitting parameter a, b, and $\langle wRH \rangle$, respectively. Thus error in the estimated R(RH) are

$$\frac{\Delta R(\mathrm{RH})}{R(\mathrm{RH})} = \left[\frac{1}{R(\mathrm{RH})} \cdot a(1 + \varepsilon_a)\right.$$
$$\left.\cdot \{1 - \langle wRH \rangle(1 + \varepsilon_{\langle wRH \rangle})\}^{-b(1+\varepsilon_b)}\right] - 1, \quad (\mathrm{A7})$$

where ε_a, ε_b, and $\varepsilon_{\langle wRH \rangle}$ are relative error in a, b and $\langle wRH \rangle$, respectively. The ranges of Δa and Δb (± 0.07 and ± 0.08, respectively) are shown in the gray dotted lines in Figure 4. The range of $\Delta\langle wRH \rangle$ was estimated to be less than 5%, based on the calculation from ± 1 standard deviation of all the RH data in each level-leg. This magnitude of $\Delta\langle wRH \rangle$ is correspond to $|\varepsilon_{\langle wRH \rangle}| \leq 0.1$. Thus $\Delta R(\mathrm{RH})/R(\mathrm{RH})$ is inferred to be less than 10% and less than 20% when $\varepsilon_{\langle wRH \rangle} = -0.1$ and $\varepsilon_{\langle wRH \rangle} = +0.1$, respectively, according to equation (A7). When these errors are convoluted, $\Delta R(\mathrm{RH})/R(\mathrm{RH})$ grows as large as 30% for the given ranges of Δa, Δb, and $\Delta\langle wRH \rangle$.

References

Anderson, T. L., and J. A. Ogren (1998), Determining aerosol radiative properties using the TSI 3563 integrating nephelometer, *Aerosol Sci. Technol.*, 29, 57–69.

Andrews, E., P. J. Sheridan, J. A. Ogren, and R. Ferrare (2004), In situ aerosol profiles over the Southern Great Plains cloud and radiation test bed site: 1. Aerosol optical properties, *J. Geophys. Res.*, 109, D06208, doi:10.1029/2003JD004025.

Bréon, F.-M., D. Tanré, and S. Generoso (2002), Aerosol effect on cloud droplet size monitored from satellite, *Science*, 295, 834–838.

Charlson, R. J., D. S. Covert, and T. V. Larson (1984), Observation of the effect of humidity on light scattering by aerosols, in *Hygroscopic Aerosols*, edited by L. H. Ruhnke and A. Deepak, A. Deepak, Hampton, Va., 375 p.

Charlson, R. J., J. Langner, H. Rodhe, C. B. Leovy, and S. G. Warren (1991), Perturbation of the northern hemisphere radiative balance by back scattering from anthropogenic sulfate aerosols, *Tellus, Ser. B*, 43, 152–163.

Covert, D. S., R. J. Charlson, and N. C. Ahlquist (1972), A study of the relationship of chemical composition and humidity to light scattering by aerosols, *J. Appl. Meteorol.*, 11, 968–976.

Damoah, R., N. Spichtinger, C. Forster, P. James, I. Mattis, U. Wandinger, S. Beirle, T. Wagner, and A. Stohl (2004), Around the world in 17 days—Hemispheric-scale transport of forest fire smoke from Russia in May 2003, *Atmos. Chem. Phys.*, 4, 1311–1321.

Feingold, G. (2003), Modeling of the first indirect effect: Analysis of measurement requirements, *Geophys. Res. Lett.*, 30(19), 1997, doi:10.1029/2003GL017967.

Feingold, G., and B. Morley (2003), Aerosol hygroscopic properties as measured by lidar and comparison with in situ measurements, *J. Geophys. Res.*, 108(11), 4327, doi:10.1029/2002JD002842.

Feingold, G., W. L. Eberhard, D. E. Veron, and M. Previdi (2003), First measurements of the Twomey aerosol indirect effect using ground-based remote sensors, *Geophys. Res. Lett.*, 30(6), 1287, doi:10.1029/2002GL016633.

Feingold, G., R. Furrer, P. Pilewskie, L. A. Remer, Q. Min, and H. Jonsson (2006), Aerosol indirect effect studies at Southern Great Plains during the May 2003 intensive operations period, *J. Geophys. Res.*, 111, D05S14, doi:10.1029/2004JD005648.

Ferrare, R., et al. (2006), Evaluation of daytime measurements of aerosols and water vapor made by an operational Raman lidar over the Southern Great Plains, *J. Geophys. Res.*, 111, D05S08, doi:10.1029/2005JD005836.

Ferrare, R., G. Feingold, S. Ghan, J. Ogren, B. Schmid, S. E. Schwartz, and P. Sheridan (2006), Preface to special section: Atmospheric Radiation Measurement Program May 2003 Intensive Operations Period examining aerosol properties and radiative influences, *J. Geophys. Res.*, 111, D05S01, doi:10.1029/2005JD006908.

Gasso, S., et al. (2000), Influence of humidity on the aerosol scattering coefficient and its effect on the upwelling radiance during ACE-2, *Tellus*, 52B, 546–567.

Hänel, G. (1976), The properties of atmospheric aerosol particles as functions of the relative humidity at thermodynamic equilibrium with the surrounding moist air, *Adv. Geophys.*, 19, 73–188.

Hegg, D. A., T. Larson, and P. Yuen (1993), A theoretical study of the effects of relative humidity on light scattering by tropospheric aerosols, *J. Geophys. Res.*, 98, 18,435–18,439.

Hegg, D. A., D. S. Covert, M. J. Rood, and P. V. Hobbs (1996), Measurements of aerosol optical properties in marine air, *J. Geophys. Res.*, 98, 12,893–12,903.

Hegg, D. A., J. Livingston, P. V. Hobbs, T. Novakov, and P. Russell (1997), Chemical apportionment of aerosol column optical depth off the mid-Atlantic coast of the United States, *J. Geophys. Res.*, 102(D21), 25,293–25,303.

Holben, B. N., et al. (1998), AERONET—a federated instrument network and data archive for aerosol characterization, *Remote Sens. Environ.*, 66, 1–16.

Ignatov, A., and N. R. Nalli (2002), Aerosol retrievals from multi-year multi-satellite AVHR Pathfinder Atmosphere (PATMOS) dataset for correcting remotely sensed sea surface temperatures, *J. Atmos. Oceanic Technol.*, 19, 1986–2008.

Jaffe, D., I. Bertschi, L. Jaegle, P. Novelli, J. S. Reid, H. Tanimoto, R. Vingarzan, and D.L. Westphal (2004), Long-range transport of Siberian biomass burning emissions and impact on surface ozone in western North America, *Geophys. Res. Lett.*, 31, L16106, doi:10.1029/2004GL020093.

Jeong, M.-J., and Z. Li (2005), Quality, compatibility and synergy analyses of global aerosol products derived from the advanced very high resolu-

tion radiometer and total ozone mapping spectrometer, *J. Geophys. Res.*, 110, D10S08, doi:10.1029/2004JD004647.

Jeong, M.-J., Z. Li, D. A. Chu, and S.-C. Tsay (2005), Quality and compatibility analyses of global aerosol products derived from the advanced very high resolution radiometer and moderate resolution imaging spectroradiometer, *J. Geophys. Res.*, 110, D10S09, doi:10.1029/2004JD004648.

Kasten, F. (1969), Visibility in the phase of pre-condensation, *Tellus*, 21, 631–635.

Kaufman, Y. J., and T. Nakajima (1993), Effect of Amazon smoke on cloud microphysics and albedo—Analysis from satellite imagery, *J. Appl. Meteorol.*, 32, 729–744.

Kaufman, Y. J., et al. (2005), A critical examination of the residual cloud contamination and diurnal sampling effects on MODIS estimates of aerosol over ocean, *IEEE Trans. Geosci. Remote Sens.*, 43(12), 2886–2897.

Kaufman, Y. J., I. Koren, L. A. Remer, D. Rosenfeld, and Y. Rudich (2005), The effect of smoke, dust, pollution aerosol on shallow cloud development over the Atlantic Ocean, *Proc. Natl. Acad. Sci. U. S. A.*, 102(32), 11,207–11,212.

Koren, I., Y. J. Kaufman, L. A. Remer, D. Rosenfeld, and Y. Rudich (2005), Aerosol invigoration and restructuring of Atlantic convective clouds, *Geophys. Res. Lett.*, 32, L14828, doi:10.1029/2005GL023187.

Kotchenruther, R. A., and P. V. Hobbs (1998), Humidification factors of aerosols from biomass burning in Brazil, *J. Geophys. Res.*, 103(24), 32,082–32,089.

Kotchenruther, R. A., P. V. Hobbs, and D. A. Hegg (1999), Humidification factors for atmospheric aerosols off the mid-Atlantic coast of the United States, *J. Geophys. Res.*, 104(2), 2239–2251.

Lesins, G., P. Chylek, and U. Lohmann (2002), A study of internal and external mixing scenarios and its effect on aerosol optical properties and direct radiative forcing, *J. Geophys. Res.*, 107(10), 4094, doi:10.1029/2001JD000973.

Li, J., J. G. D. Wong, J. S. Dobbie, and P. Chýlek (2001), Parameterization of the optical properties of sulfate aerosols, *J. Atmos. Sci.*, 58, 193–209.

Li-Jones, X., H. B. Maring, and J. M. Prospero (1998), Effect of relative humidity on light scattering by mineral dust aerosol as measured in the marine boundary layer over the tropical Atlantic Ocean, *J. Geophys. Res.*, 103(23), 31,113–31,121.

Myhre, G. F., et al. (2004), Intercomparison of satellite retrieved aerosol optical depth over ocean, *J. Atmos. Sci.*, 61, 499–513.

Nakajima, T., A. Higurashi, K. Kawamoto, and J. E. Penner (2001), A possible correlation between satellite-derived cloud and aerosol microphysical parameters, *Geophys. Res. Lett.*, 28, 1171–1174.

Öström, E., and K. J. Noone (2000), Vertical profiles of aerosol scattering and absorption measured in situ during the North Atlantic Aerosol Characterization Experiments, *Tellus, Ser. B*, 52, 526–545.

Pahlow, M., G. Feingold, A. Jefferson, E. Andrews, J. A. Ogren, J. Wang, Y.-N. Lee, R. A. Ferrare, and D. D. Turner (2006), Comparison between lidar and nephelometer measurements of aerosol hygroscopicity at the Southern Great Plains Atmospheric Radiation Measurement site, *J. Geophys. Res.*, 111, D05S15, doi:10.1029/2004JD005646.

Remer, L. A., S. Gasso, and D. A. Hegg (1997), Urban/industrial aerosol: Ground-based Sun/sky radiometer and airborne in situ measurements, *J. Geophys. Res.*, 102, 16,849–16,859.

Rood, M. J., D. S. Covert, and T. V. Larson (1987), Hygroscopic properties of atmospheric aerosol in Riverside, California, *Tellus, Ser. B*, 39, 383–397.

Sheridan, P. J., D. J. Delene, and J. A. Ogren (2001), Four years of continuous surface aerosol measurements from the Department of Energy's Atmospheric Radiation Measurement Program Southern Great Plains Cloud and Radiation Testbed site, *J. Geophys. Res.*, 106, 20,735–20,747.

Tang, I. N. (1996), Chemical and size effects of hygroscopic aerosols on light scattering coefficients, *J. Geophys. Res.*, 101(D14), 19,245–19,250, doi:10.1029/95JD03003.

Turner, D. D., R. A. Ferrare, and L. A. Brasseur (2001), Average aerosol extinction and water vapor profiles over the Southern Great Plains, *Geophys. Res. Lett.*, 28(23), 4441–4444.

Wang, J., S. A. Christopher, U. S. Nair, J. S. Reid, E. M. Prins, J. Szykman, and J. L. Hand (2006), Mesoscale modeling of Central American smoke transport to the United States: 1. "Top-down" assessment of emission strength and diurnal variation impacts, *J. Geophys. Res.*, 111, D05S17, doi:10.1029/2005JD006416.

————————

E. Andrews, Climate Monitoring and Diagnostics Laboratory, National Oceanic and Atmospheric Administration, Boulder, CO, USA.

M.-J. Jeong and Z. Li, Department of Atmospheric and Oceanic Science and Earth System Science Interdisciplinary Center, University of Maryland, College Park, MD 20742, USA. (mjeong@climate.gsfc.nasa.gov)

S.-C. Tsay, Laboratory for Atmospheres, NASA Goddard Space Flight Center, Greenbelt, MD, USA.